Received August 29, 2019, accepted September 12, 2019, date of publication September 20, 2019, date of current version October 16, 2019.

Digital Object Identifier 10.1109/ACCESS.2019.2942524

Simulation of Road Capacity Considering the Influence of Buses

JINXING SHEN[1], JUNJIE QI[1], FENG QIU[2], AND CHANGJIANG ZHENG[1]
[1]College of Civil and Transportation Engineering, Hohai University, Nanjing 210096, China
[2]Department of Computer Science, University of Victoria, Victoria, BC V8W3P6, Canada

Corresponding author: Jinxing Shen (shenjx03@163.com)

This work was supported in part by the National Natural Science Foundation of China under Grant 51808187, in part by the Natural Science Foundation of Jiangsu Province under Grant BK20170879, in part by the Fundamental Research Funds for the Central Universities under Grant 2019B13514, and in part by the Jiangsu Planned Projects for Postdoctoral Research Funds under Grant 1701086B.

ABSTRACT The traditional cellular automata model cannot fully demonstrate the effect of buses on road capacity due to the incapable of considering the difference in dynamic performance and driving behaviors between buses and other vehicles. In this paper, a novel cellular automata model accounting for car-following and lane-changing behaviors was developed to investigate the relationship between the multilane road capacity and the proportion of buses. The parameters of the model were calibrated and verified using the data collected from a real-word road with heterogeneous traffic flow. The calibration result indicates that the proposed model can accurately describe the evolution of traffic dynamics on multilane roads. It is found that drivers have a specific preference in determining the target lane in the lane-changing process. Under the same conditions, bus drivers prefer to choose the side lane of the road, while drivers of other vehicles prefer to select the middle lanes. Besides, the preference for the target lanes affects the lane-changing behaviors of the drivers, resulting in a considerable difference in optimal traffic density and maximum traffic volume in different lanes. Moreover, the simulation result suggests that the proportion of buses has a significant impact on road capacity (e.g., the capacity is reduced by as much as 18%). To increase road capacity and improve bus services, based on the proposed model, transit authorities can dynamically allocate the limited road space to buses and other vehicles according to the proportion of buses.

INDEX TERMS Multilane road capacity, cellular automata model, car-following, lane-changing, bus.

I. INTRODUCTION

Road capacity can be derived from the correlations between three key traffic variables, namely, flow, speed, and density [1]. However, there is no easy way to measure the road capacity in the field or estimate the road capacity under different traffic conditions [2]. The previous studies have shown that road capacity depends on traffic composition, varies greatly from lane to lane, and falls by $8 \sim 9\%$ through traffic breakdown [3]–[10]. The road capacity is often underutilized due to the inefficiency of ramp metering control [11]. The *Highway Capacity Manual* (HCM) provides an authoritative source of static data on road capacity [12]. But road capacity is a variable that changes with the local conditions [13].

The first step to quantify the variation in road capacity is to understand the complex features of multilane traffic. Many scholars have attempted to identify these features. For instance, Kerner et al. developed a simple cellular automaton model for road capacity in two-lane roads [14], and explored the effect of automatic vehicles on mixed traffic flow, using the three-phase traffic theory [15]. Ameri et al. designed neural networks (NNs) to evaluate the capacity of two-lane roads in the suburbs [16]. Tang et al. created a macro traffic flow model to disclose how road capacity affects traffic flow [17]. Qian et al. improved the cellular automaton model to investigate the effects of a multi-point tollbooth on traffic flow [18]. Chen et al. estimated the capacity of urban expressway through microscale simulation [19]. He and Jia et al. combined the empirical data with traffic flow theory, and successfully simulated road capacity [20]–[22]. However, the above studies have not included speed and acceleration limits of different vehicles in the simulation models.

The previous studies have also shown that road capacity may be reduced by the lane-changing maneuvers of buses.

The associate editor coordinating the review of this manuscript and approving it for publication was Sabah Mohammed.

Despite taking up a small fraction of the traffic flow, the buses have a great impact on road capacity, especially under heavy traffic. Unfortunately, previous simulation modeling always translates buses into equivalent passenger car units, which couldbuses inadequately depict the road capacity reduction phenomenon caused by buses within the real traffic flow. Therefore, it is necessary to develop a multilane simulation model to consider the interactions between buses and other vehicles when analysis the fluctuation of road capacity. With the help of the model, we could effectively allocate limited road space to buses and other vehicles, and provide reliable public transit service while increasing the maximum traffic volume.

The remainder of this paper is organized as follows: Section 2 develops a multilane cell transmission model that simulates the driving behaviors of various vehicles on multilane roads; Section 3 calibrates the variables of the established model with field data; Section 4 carries out simulations under different compositions of traffic flow; Section 5 puts forward the research conclusions.

II. MODEL FORMULATION

On multilane roads, the driving behaviors of various vehicles directly bear on the heterogeneity of the traffic flow. These behaviors, e.g. car-following and lane-changing, must be simulated before designing a model of the multilane traffic. In fact, the decisions on car-following and lane-changing are affected by the heterogeneous traffic flow, as well as external factors like road geometry and traffic control plan. Therefore, this section develops a multilane cell transmission model to simulate the microscale traffic state in temporal, longitudinal and lateral dimensions. The model consists of a traffic flow module that governs the traffic flow propagation in each lane, and an acceptance mechanism for car-following and lane-changing based on gap assessment rules. The flow chart of the established model is illustrated in Fig 1 below.

The multilane cell transmission model can be implemented in the following steps:

Step 1: Initializing the simulation variables: set the initial and final positions, input the start and end times, and configure the driver variables, road variables (land width, lane length, the number of lanes, etc.), and vehicle variables (vehicle sizes, speed limits, acceleration/deceleration limits, etc.).

Step 2: Determining the traffic state: design the traffic management strategy of each lane, the vehicle speed, gap, and driver status at time t.

Step 3: Selecting the suitable lane and driving behaviors: the driver of each vehicle selects a suitable lane based on the traffic state, i.e. choose between car-following and lane-changing, and then determines the suitable acceleration or deceleration.

Step 4: Updating vehicle positions and detection data: Compute the actual speed of each vehicle, and update the time and position of each vehicle and the traffic flow.

A. POSITION UPDATE UNDER CAR-FOLLOWING STATE

Let x_n be the position of a vehicle at time t_n. Since the time step τ of is constant, time t_n can be expressed as:

$$t_n = n\tau \quad s.t.\ n = 1, 2, \ldots, \frac{T}{\tau} \tag{1}$$

where n is the time index of t_n; T is the total simulation time. In the subsequent time t_{n+1}, the relationship between vehicle speed and position can be described as:

$$f(v, x) \overset{def}{=} \begin{cases} v_{n+1} = \max(0, v(\min)) \\ x_{n+1} = x_n + v_{n+1}\tau \\ v(\min) = \min(v_{free,l}, v_{m,n}, v_{r,n}, v_{c,n}) \end{cases} \tag{2}$$

where $v_{free,l}$ is the maximum free-flow speed of vehicles depending on the vehicle performance and speed limit of each lane l; $v_{m,n}$ is the maximum safe speed of vehicles depending on vehicle position and the gap between the current vehicle and the leading vehicle; $v_{r,n}$ is the vehicle speed under random fluctuation state depending on the driver emotions:

$$v_{r,n} = v_{n-1} + a_{m,n}\tau\eta_n \tag{3}$$

where v_{n-1} is the vehicle speed at time t_{n-1}; $a_{m,n}$ is the maximum acceleration/deceleration of vehicles at time t_n; η_n are normally distributed random variables; $v_{c,n}$ is the maximum possible speed of vehicles in the car-following state:

$$\begin{cases} v_{c,n} = v_{n-1} + \ddot{x}_{c,n} \times \tau \\ \ddot{x}_{c,n} = \beta_{0,c} G_{l,n,c}^{\beta_{1,c}} \times (\frac{\dot{x}_{f,n}}{\dot{x}_{s,n}})^{\beta_{2,c}} \times (\ddot{x}_{f,n-1})^{\beta_{3,c}} \end{cases} \tag{4}$$

where $\ddot{x}_{c,n}$ is the possible acceleration/deceleration of the current vehicle; $G_{l,n,c}$ is the gap between the current vehicle and the leading vehicle at time t_n; $\dot{x}_{f,n}$ and $\dot{x}_{s,n}$ are the speeds of the front vehicle and the current vehicle at time t_n, respectively; $\ddot{x}_{f,n-1}$ is the acceleration/deceleration of the leading vehicle at time t_{n-1}; $\beta_{0,c}$, $\beta_{1,c}\beta_{2,c}$ and $\beta_{3,c}$ are the correlation coefficients, defined by Shen *et al.* [23], for the explanatory variable of equation (4).

B. POSITION UPDATE UNDER LANE-CHANGING STATE

The lane-changing often leads to stop-and-go waves in the upper lane. This maneuver must be well simulated by the multilane traffic model. The previous studies have found that fewer buses in traffic flow helps reduce the collision risk induced by lane-changing behavior, and young female drivers are more likely to cause collisions in lane-changing than male drivers. The accurate modelling of lane-changing behavior is critical to the safety of vehicles.

The utility of lane l perceived by driver n at time t can be expressed as [24]:

$$U_{ltn} = V_{ltn} + \varepsilon_{ltn} \quad \forall l \in L_n \tag{5}$$

where V_{ltn} is the utility of lane l reflected by the traffic environment; L_n is the set of adjacent lanes that can be selected by driver n; ε_{ltn} is an independent, normally-distributed, random utility component of lane l perceived by driver n at time t.

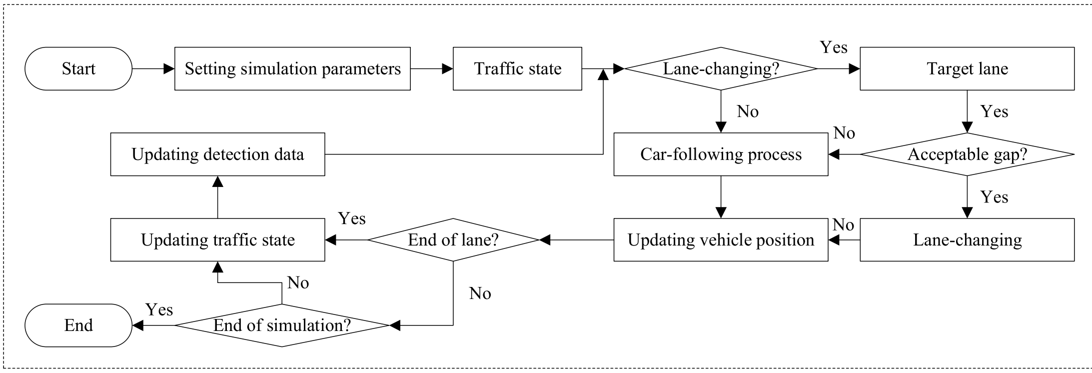

FIGURE 1. Flow chart of multilane cell transmission model.

According to Choudhury, the utility of the target lane is affected by the features of the lane, the features of the adjacent vehicles in the lane, and the driving plan. Therefore, the utility of the target lane under the discretionary lane-changing can be described as:

$$V_{ltn} = \beta_0^l + \beta_1^l D_{ltn} + \beta_2^l V_{ltn}^{avg} + \beta_3^l \Delta X_{ltn}^{front} + \beta_4^l \Delta V_{lt}^{front} + \alpha^l v_n \quad (6)$$

where β_0^l (pcu/km) is a fixed term in the utility function of lane l; D_{ltn} is the density of lane l; V_{ltn}^{avg}(m/s) is the average speed in lane l; ΔX_{ltn}^{front} (m) and ΔV_{ltn}^{front} (m/s) are the lead gap and lead speed between the current vehicle and the leading vehicle in lane l, respectively; β_i^l is the correlation coefficient vector of the explanatory variable of the utility function; $v_n \sim N(0, 1)$ is a random error term generated by the features of the driver; α^l is the correlation coefficient vector of v_n. Note that the lead gap refers to the distance between the front of the current vehicle and the rear of the leading vehicle in lane l and the lead speed refers to the speed difference between the current vehicle and the leading vehicle in lane l.

It is assumed that the random error terms in the utility functions of different lanes are independent in terms of distribution. Then, the probability that driver n selects lane l can be expressed as:

$$P_{tn}(l_t|v_n) = \frac{\exp(V_{ltn}|v_n)}{\sum\limits_{l_i \in L_n} \exp(V_{l_i tn}|v_n)} \quad \forall l, l_i \in L_n \quad (7)$$

It is also assumed that the lane with the highest probability is the target lane of lane-changing. Based on Choudhury's model, the utility function of our lane-changing model can be derived from the gap and speed difference between the current vehicle and the leading vehicle:

$$\begin{aligned} V_{ltn} = \beta_0^l + \beta_1^l V_n + \beta_2^l V_{ltn}^{avg} + \beta_3^l D_{ltn} \\ + \beta_4^l \Delta X_{ltn}^{front} + \beta_5^l \Delta V_{ltn}^{front} + \beta_6^l \Delta X_{ltn}^{lag} \\ + \beta_7^l \Delta V_{ltn}^{lag} + \alpha^l v_n \end{aligned} \quad (8)$$

where V_n is the speed of the current vehicle n in the current lane; $V_{ltn}^{avg}(m/s)$ is the average speed of lane l; ΔX_{ltn}^{front} (m) and $\Delta V_{ltn}^{front}(m/s)$ are the lead gap and lead speed between the current vehicle and the leading vehicle in lane l, respectively; $\Delta X_{ltn}^{lag}(m)$ and $\Delta V_{ltn}^{lag}(m/s)$ are the lag gap and lag speed between the current vehicle and the lagging vehicle in lane l, respectively; β_i^l is the correlation coefficient vector of the explanatory variable of the utility function ($i = 1, 2, \cdots 7$). Note that the lag gap refers to the distance between the rear of the current vehicle and the front of the lagging vehicle in lane l and the lead speed refers to the speed difference between the current vehicle and the lagging vehicle in lane l.

After selecting the most suitable lane to change, the driver should evaluate the available adjacent gap in the target lane and decide whether to change lanes immediately. The gap must be greater than the critical lead or lag gaps below:

$$\ln(G_{\ln t}) = \beta X_{\ln t} + \alpha v_n + \varepsilon_{\ln t} \quad (9)$$

where $G_{\ln t}$ is the critical gap in the direction of target lane $l(m)$; $X_{\ln t}$ is the explanatory variable that affects either the critical lead gap or critical lag gap in the direction of the target lane l; α is the lead/lag gap acceptance coefficient of individual-specific explanatory variable v_n; $\varepsilon_{\ln t} \sim N(0, \sigma^2)$ are random terms.

III. CALIBRATION OF SIMULATION VARIABLES

The field data were collected from Xuanwu Avenue, a four-lane road that stretches from west to east in downtown Nanjing, China, using microwave radar detector and roadside laser detector. The trajectories of different vehicles in the road section were simulated, and used to compute the speeds and accelerations. The computed results were adopted to estimate our model for lane-changing. The variables of each lane, including lane density, lane speed, and the proportion of buses, were derived from the raw data. The resulting estimation data contain 2,888 entries on 815 lane-changing vehicles. About 40% of the data were categorized as calibration data and the rest as the test data. Overview of the data are shown in Table 1.

Fig. 2 presents the effects of the level of service (LOS), which covers traffic flow, speed, delay and safety, on a

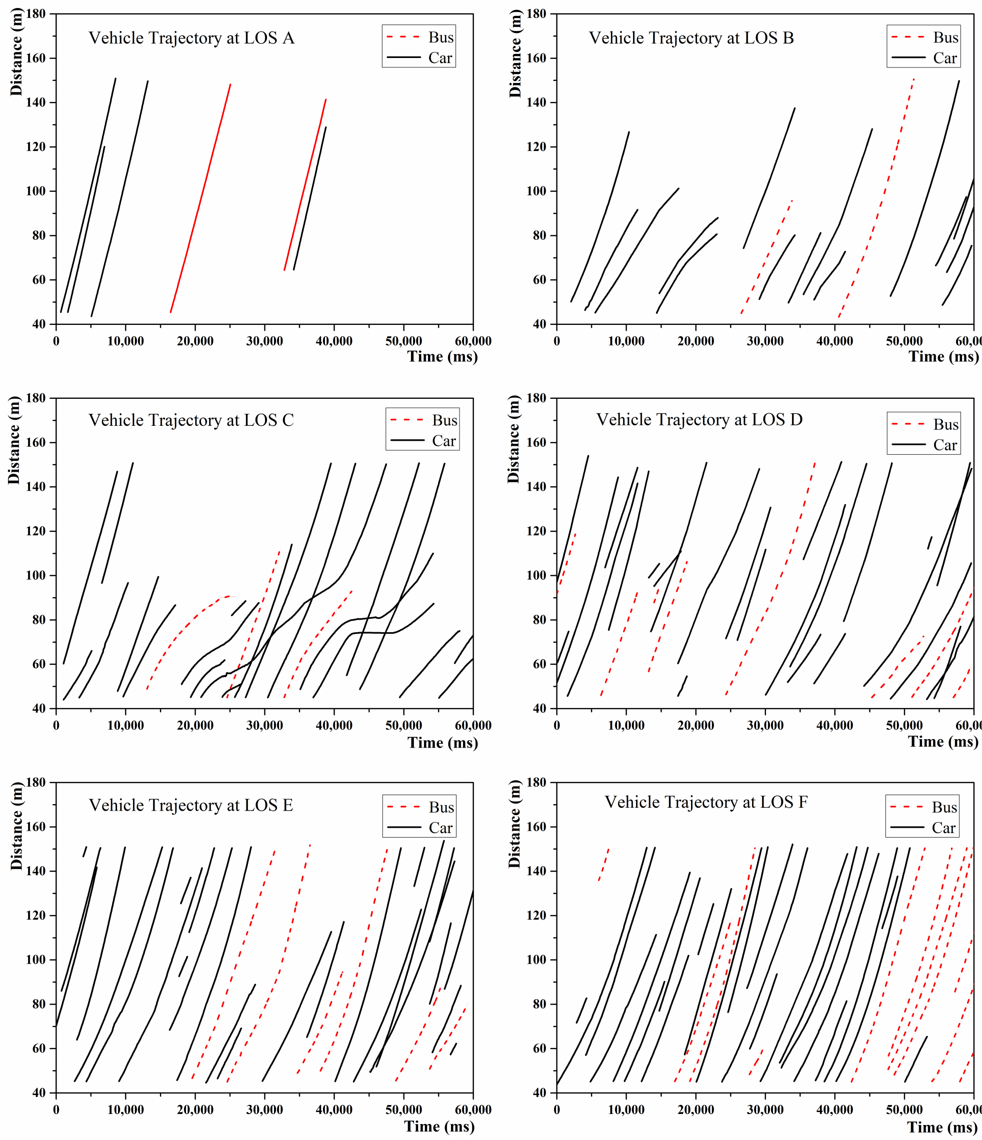

FIGURE 2. The trajectories at different LOSs.

TABLE 1. Overview of the research data.

Data source	Xuanwu Avenue, Nanjing, China		
	7~9am, April 13th, 2016		
	Lane-changing	No lane-changing	Total
Calibration data	326	2,562	2,888
Test data	489	3,842	4,331
Total	815	6,404	7,219

Note: Details on the research data are available in Reference [23].

specific lane of the multilane road. It can be seen that the lane-changing behavior varies significantly with the LOSs. Also, the trajectories show that the lane-changing behavior is obviously affected by the operation features and traffic flow of the multilane road.

In Fig. 2, The lane-changing behavior occurs frequency at LOS C. When the LOS belongs to classes A and B, each vehicle tends to drive on the current lane, because of the high degree of freedom to select speed and operating conditions of each lane. However, the traffic flow does not increase at the same rate across the adjacent lanes of the multilane road. Thus, the drivers on different lanes tend to change lanes for a better driving experience. When the LOS is above class C, there is often few acceptable gaps in the target lane, which suppresses the lane-changing behavior. Thus, the lane-changing behaviors at LOS C were selected to analyze the drivers' preference on lane-changing behavior.

A. CALIBRATION OF CAR-FOLLOWING VARIABLES

Before calibrating car-following variables, the field data were divided into two parts. Each part was further split

TABLE 2. Variables fitting results.

Group name		β_0	β_1	β_2	β_3	R^2
B-B	Acceleration	0.2245	0.6511	0.5257	0.0001	0.83
	Deceleration	0.7418	-0.1522	0.8485	0.0003	0.72
C-C	Acceleration	5.3197	-1.6116	4.8996	0	0.62
	Deceleration	30.368	-1.593	-0.4587	-0.1221	0.65
C-B	Acceleration	35.357	-1.3156	0.5439	0.0003	0.84
	Deceleration	0.0001	3.1173	-0.7944	-0.1906	0.7
B-C	Acceleration	0.1242	1.0699	0.2817	0.0001	0.64
	Deceleration	38.303	-2.235	-0.2705	0.1222	0.89

into 8 groups based on acceleration, deceleration, and four vehicle-following patterns, namely, car following car (C-C), car following bus (C-B), bus following bus (B-B) and bus following car (B-C). Variables of equation (4) were fitted by maximum likelihood estimation (in Reference [23]) and the results are displayed in Table 2.

B. BCALIBRATION OF LANE-CHANGING VARIABLES

This subsection calibrates the explanatory variables of (4) by the maximum likelihood estimation. The likelihood curve is not purely concave. If all coefficients of the individual-specific error term have opposite signs, then the solution will not change because of the symmetricity of the curve. To prevent falling into the local optimum trap, multiple points were selected for the optimization. Note that the estimation involves no traffic simulator, i.e. the estimated models are simulator-independent.

1) CRITICAL GAP OF LANE-CHANGING

A vehicle cannot change into the target lane if the available gap is not acceptable. Before lane-changing, the driver must evaluate the adjacent gap in the target lane and decide whether to change lanes immediately. Besides, both lead and lag gaps should be greater than the corresponding critical gaps before changing lanes.

During lane-changing, the critical lead and lag gaps are not fixed values, but vary with the speed of the current vehicle in the current lane and that of the vehicles in the adjacent lane. The relationship between the critical gaps and the speed difference was derived from the trajectories in lane-changing (Fig. 3).

Based on exponential model, the relationship between the critical gaps and speed differences can be expressed as:

$$\begin{cases} G_{lead} = 4.11e^{0.3859V_{dlead}} + 12.14 \\ G_{lag} = 15.63e^{0.1683V_{dlag}} \end{cases} \tag{10}$$

where G_{lead} is the critical gap between the current vehicle n on original lane and the leading vehicle on adjacent lane; G_{lag} is the gap between the current vehicle n on original lane and the lagging vehicle on adjacent lane; V_{dlead} is the speed difference between the current vehicle n on original

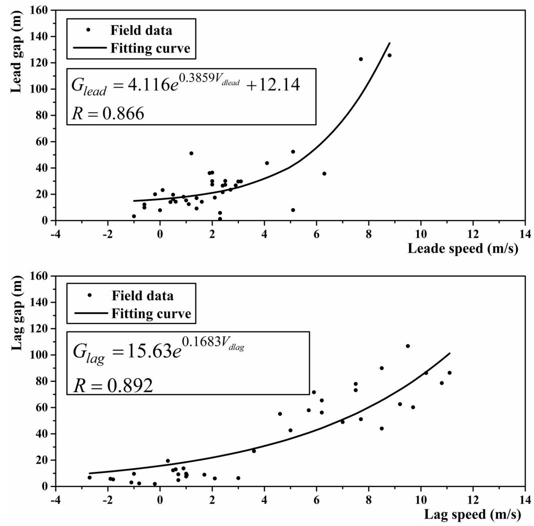

FIGURE 3. Speed difference under lane-changing process.

lane and the leading vehicle on adjacent lane; V_{dlag} is the speed difference between the current vehicle n on original lane and the lagging vehicle on adjacent lane.

It can be seen from equation (10) that, in the course of lane-changing, drivers differ in their requirements on the gap between adjacent lanes. Under the same speed difference, the critical lead gap is generally larger than the critical lag gap. Besides, the two critical gaps grow at different rates with the increase in speed difference.

2) MODEL CALIBRATION

The likelihood function was employed to describe the lane-changing decision of the driver on the multilane road. It is assumed that different drivers are independent in their observations. The explanatory variables of equation (8) were computed by the maximum likelihood estimates on MATLAB.

The 815 pairs of lane-changing trajectories were split into two groups: 326 pairs for calibration and 489 pairs for testing. The calibration results of our model and Choudhury's model were given in Tables 3 and 4, respectively. Since the Sig values were less than 0.05, the variables of the two models are statistically significant in the calibration process.

3) PERFORMANCE COMPARISON

The receiver operating characteristic (ROC) curve of our model were compared with that of Choudhury's model. Both curves were drawn based on the 489 pairs of trajectories for testing. The ROC curves of two models are shown in Fig 4.

The ability of each model to predict the selected lane can be determined easily by comparing its ROC curve with a straight line with a slope of 45°. The larger the area between the curve and the line, the stronger the prediction ability of the model, that is, the smaller the false positive and negative prediction results. The area under the ROC curve generally falls between 0.5 and 1.0. The prediction ability increases

TABLE 3. Calibration results of our model.

Variables	Calibration results	S.E.	Wald	df	Sig.	Exp (B)
β_1^l	0.593	0.014	3.572	1	0.009	1.809
β_2^l	0.117	0.103	1.297	1	0.025	1.124
β_3^l	-0.096	0.036	7.009	1	0.008	0.909
β_4^l	0.031	0.023	1.802	1	0.019	1.032
β_5^l	0.782	0.072	8.277	1	0.004	2.186
β_6^l	0.076	0.040	3.610	1	0.027	1.079
β_7^l	-0.128	0.244	0.275	1	0.000	0.880
β_0^l	-7.720	4.046	3.640	1	0.036	0.000

Note: S.E. is short for standard error; Wald refers to the result of the Wald Chi-Squared Test on whether the overall regression coefficient is zero; df stands for degree of freedom of the Wald Chi-Squared Test; Sig. means the significance of the calibration results; Exp (B) is the exponential form of the calibration results, indicating the change rate in time when one factor changes by one unit while the other factors remain constant.

TABLE 4. Calibration results of Choudhury's model.

Variables	Calibration results	S.E.	Wald	df	Sig.	Exp (B)
β_1^l	-0.029	0.016	3.254	1	0.031	0.972
β_2^l	0.105	0.075	1.968	1	0.000	1.111
β_3^l	0.008	0.010	0.629	1	0.042	1.008
β_4^l	0.496	0.141	12.327	1	0.000	1.642
β_0^l	-3.777	2.803	1.816	1	0.017	0.023

Note: The indices have the same meanings with those in Table 3.

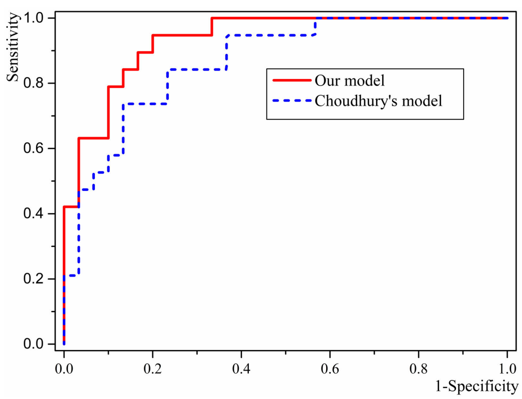

FIGURE 4. The ROC curves of our model and Choudhury's model.

as the area approaches 1.0. If the area is smaller than 0.5, the model is inapplicable; if the area is equal to 0.5, the model is invalid; if the area is between 0.5 and 0.7, the model has a poor prediction accuracy; if the area is between 0.7 and 0.9, the model has a medium accuracy; if the area is greater than 0.9, the model has a high accuracy. Based on the trajectories, the ROC curves of the two models were compared in Table 5.

TABLE 5. Comparison of the ROC curves.

Variables	Area	SE	Asymptotic Sig	Asymptotic 95% confidence interval	
				Lower limit	Upper limit
Our model	0.933	0.033	0.000	0.868	0.998
Choudhury's model	0.868	0.051	0.000	0.769	0.967

As shown in Table 5, the area under the ROC curve of our model was 0.933, larger than that of Choudhury's model (0.868). This means our model has the better prediction ability on discretionary lane-changing decisions on the multilane road.

C. MODEL VERIFICATION

In this subsection, the traffic density and traffic flow are simulated based on the actual data collected from Xuanwu Avenue. The simulation targets a 3,000m-long road section, which was divided into 6,000 cells, each corresponding to 0.5m. The four lanes of the road were denoted as Lanes 1, 2, 3 and 4, respectively, from the outside to the inside. Several detectors were arranged at the interval of 1,000 cells. During the simulation, the vehicle travelled from left to right. In the light of the field data, two types of vehicles were chosen to run on the fast lane. One is a 5m-long car, which occupies 10 cells. The other is a 12m-long bus, which occupies 24 cells. The time step was set to 1s. The proportion of buses in the traffic flow was designed as 22%, the same as the field data. The density-flow curves of different lanes were thus obtained (Fig. 5).

As shown in Fig. 5, with the growth in traffic flow, the four lanes had a marked difference in the optimal traffic density, owing to the lane-changing behaviors. Taking Lanes 1 and 4 for instance, the optimal density of Lane 1 was almost 1.6 times that of Lane 4. In addition, the four lanes suffered from a huge capacity loss induced by drivers' preference on lane selection. Taking Lanes 1 and 2 for instance, the capacity of Lane 1 was about 45% of that of Lane 2.

To verify the simulation effect of our model, the author analyzed the correlation between the traffic flows measured on Xuanwu Avenue and those simulated by our model. From the measured data, 500 sets of traffic density were randomly selected in different lanes, and used for traffic flow simulation. The measured data are compared with the simulated data in Fig. 6, where the abscissa is the measured data, the ordinate is the simulated data, the diagonal line is a reference line for the correlation of 1 (the measured data are fully consistent with the simulated data).

As shown in Fig. 6, the highest correlation (0.96) appeared in Lane 2, and the lowest (0.9) in Lane 3. The distribution of the correlation results shows that the simulated traffic flow was slightly above the measured data in Lane 3. Overall,

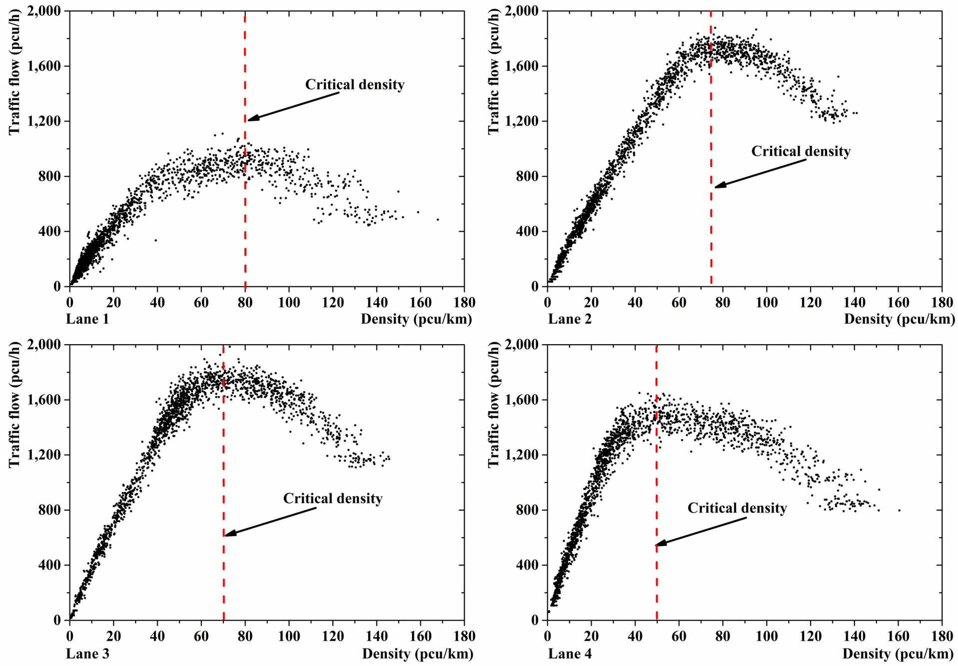

FIGURE 5. Density-flow curves of different lanes.

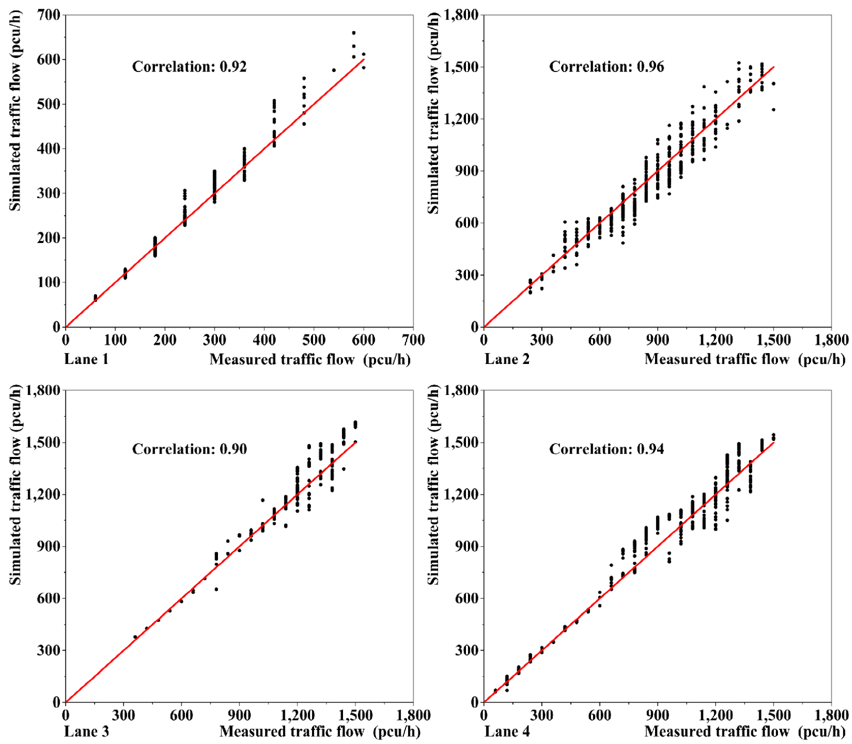

FIGURE 6. Correlation between measured and simulated traffic flows.

the correlation between measured and simulated traffic flows surpassed 0.9 in all four lanes, a sign of the applicability of our model in simulating the capacity of the target road.

IV. SIMUALTION AND RESULTS ANALYSIS

Buses and cars have great differences in space occupation, acceleration, deceleration and speed. Therefore, the

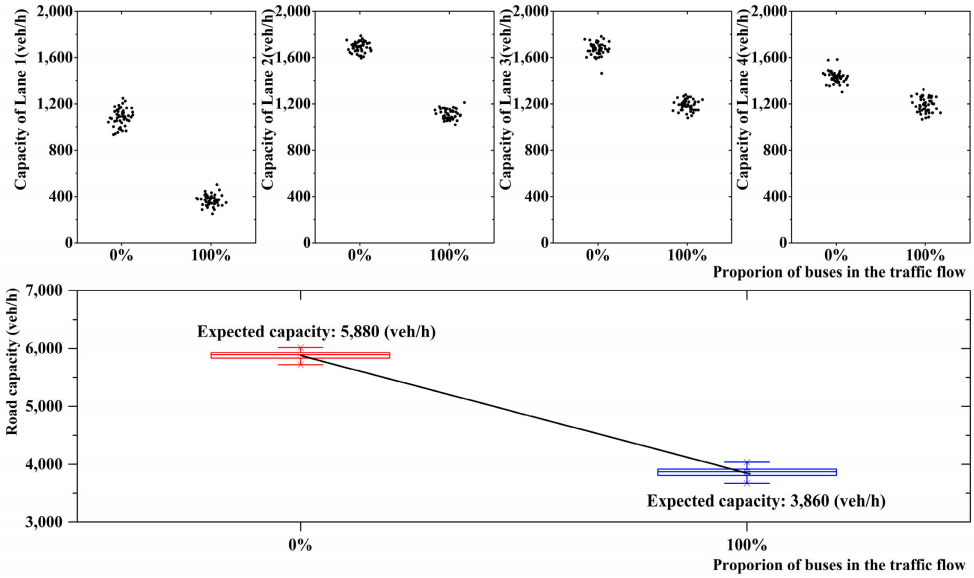

FIGURE 7. Decline in road capacity induced by buses.

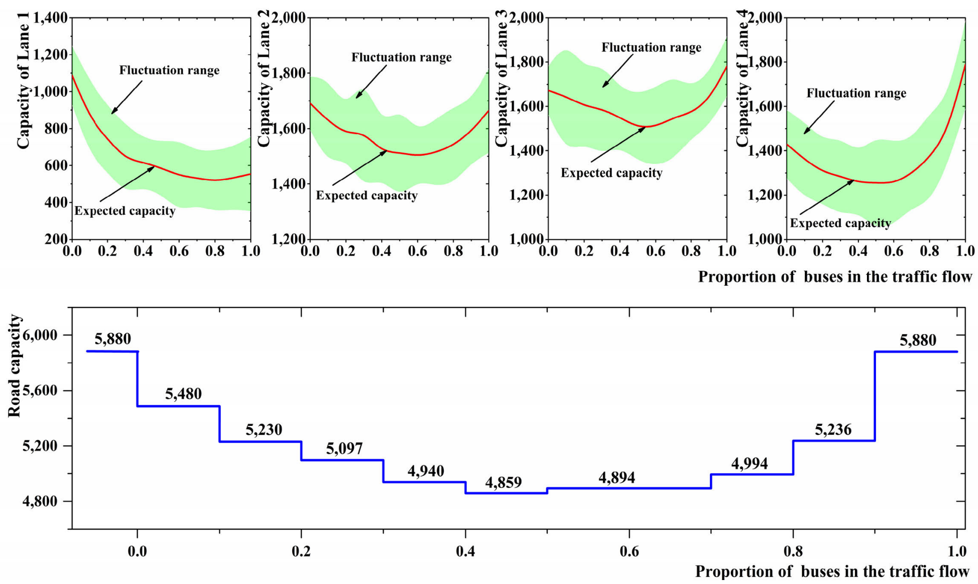

FIGURE 8. The road capacity trend with the proportions of buses.

traffic flow containing both buses and cars was converted into an equivalent flow of cars, denoted as passenger car equivalents (PCE).

To disclose the impacts of buses on road capacity, the capacity of each lane in the target road was simulated with two types of traffic flows. One of them contains only cars, and the other contains only buses. Fig. 7 illustrates the decline in road capacity induced by buses.

As shown in Fig. 7, buses caused obvious decline in road capacity, especially in Lane 1. The road capacity was expected to peak at 5,880veh/h, and minimize at 3,860veh/h, putting the difference at 2,020veh/h. The PCE of buses can be computed by:

$$PCE_{bus} = \frac{C_b}{C_c} \tag{11}$$

where C_b is the expected capacity of the pure-car traffic flow; C_c is the expected capacity of the pure-bus traffic flow. The PCE of buses were computed as 1.5 by equation (11), which agrees well with the recommended value in the *Highway Capacity Manual* (Sixth Edition, 2016). The road capacity trend with the proportions of buses is presented in Fig. 8 below.

In Fig. 8, the lane capacity changed significantly with the compositions of the traffic flow. The growing proportion of buses had the greatest impact on the capacity of Lane 1. It could be concluded that road capacity may be reduced by the lane-changing maneuvers of buses. Despite taking up a small fraction of the traffic flow, the buses have a great impact on road capacity, especially under heavy traffic. Besides, the road capacity reached the minimum level when the proportions of buses and cars were basically even. The analysis results also show that the impact of buses on multilane road capacity cannot be fully characterized by a fixed PCE of buses With the changes in the proportion of buses, the road capacity varied by 18% from the peak value of 5,880 pcu/h to the minimum value of 4,859 pcu/h. This means the impact of bus proportion must be considered in the research of road capacity.

V. CONCLUSION

This paper attempts to disclose the spatiotemporal change law of road traffic flow. Based on cellular automata model, a novel microscale model was developed to simulate car-following and lane-changing behaviors simultaneously, and to disclose how road capacity is affected by the proportion of buses. The position update rules were determined under the car-following state and the lane-changing state. Next, our model was calibrated and verified through a simulation on an actual road with heterogenous traffic flow. The main results are as follows:

The proportion of buses has a great impact on the road capacity. The four lanes had a marked difference in the optimal traffic density, owing to the lane-changing behaviors, and suffered from a huge capacity loss induced by drivers' preference on lane selection. The buses caused obvious decline in road capacity, and the growing proportion of buses had the greatest impact on the capacity of Lane 1. The capacity of that lane plunged deeply with a huge range of fluctuation. Besides, the road capacity reached the minimum level when the proportions of buses and cars were basically even. With the changes in the proportion of buses, the road capacity varied by 18% from the peak value of 5,880 pcu/h to the minimum value of 4,859 pcu/h. This means the impact of buses on multilane road capacity cannot be fully characterized by the fixed PCE of buses.

Although curbside bus stops are also proven to affect road capacity, in this study, we mainly analyze the impact of the bus on road capacity during the normal driving process, and cannot consider the bottleneck due to curbside stops of buses. Through accounting for the microscale interaction among different vehicles, our model can character the macroscale fluctuation features of actual multilane road capacity. With the proposed model, transit authorities can more intuitively understand the dynamic evolution of traffic flow and the impact of buses on the road capacity. Moreover, the research findings provide an excellent tool for transit authorities to dynamically allocate limited road space to buses and other vehicles according to the proportion of buses. Thus, transit authorities can increase road capacity while improving bus services.

REFERENCES

[1] J. Yao, H. Rakha, H. Teng, V. Kwigizile, and M. Kaseko, "Estimating highway capacity considering two-regime models," *J. Transp. Eng.*, vol. 135, no. 9, pp. 670–676, Sep. 2009.

[2] J. Kim and L. Elefteriadou, "Estimation of capacity of two-lane two-way highways using simulation model," *J. Transp. Eng.*, vol. 136, no. 1, pp. 61–66, 2010.

[3] G. Tenekeci, S. Wainaina, I. Askew, and A. Mohammad, "Sustainable operational lane capacity for highways," *Proc. Inst. Civil Eng.-Transp.*, vol. 167, no. 1, pp. 36–47, 2014.

[4] J. Shen and W. Li, "Sensitivity analysis of wavelet neural network model for short-term traffic volume prediction," *J. Appl. Math.*, vol. 2013, Dec. 2013, Art. no. 953548.

[5] Y. Zhou and P. Meng, "Diagnosis of causes for high railway traffic based on Bayesian network," *Math. Model. Eng. Problems*, vol. 6, no. 1, pp. 136–140, 2019.

[6] J. Shen, W. Li, F. Qiu, and S. Zheng, "Capacity of freeway merge areas with different on-ramp traffic flow," *Promet-Traffic Transp.*, vol. 27, no. 3, pp. 227–235, 2015.

[7] L. Leclercq, V. L. Knoop, F. Marczak, and S. P. Hoogendoorn, "Capacity drops at merges: New analytical investigations," *Transp. Res. C, Emerg. Technol.*, vol. 62, pp. 171–181, Jan. 2016.

[8] M. Guériau, F. Armetta, S. Hassas, R. Billot, and N. E. El Faouzi, "Constructivist learning based on multiagent systems. An application to the complex problem of cooperative traffic regulation," *Revue d'Intell. Artificielle*, vol. 32, no. 2, pp. 249–277, 2018.

[9] C. Wang, J. Zhang, L. Xu, L. Li, and B. Ran, "A new solution for freeway congestion: Cooperative speed limit control using distributed reinforcement learning," *IEEE Access*, vol. 7, pp. 41947–41957, 2019.

[10] S. Sugiarto, T. Limanoond, and T. Nakatsuji, "Dropped in capacity and traffic speed of urban arterial: A case study at u-turn section in Aceh province, Indonesia," *Aceh Int. J. Sci. Technol.*, vol. 1, no. 3, pp. 86–93, 2012.

[11] A. Srivastava and N. Geroliminis, "Empirical observations of capacity drop in freeway merges with ramp control and integration in a first-order model," *Transp. Res. C, Emerg. Technol.*, vol. 30, pp. 161–177, May 2013.

[12] V. Modi, A. Kondyli, S. S. Washburn, and D. S. McLeod, "Freeway capacity estimation method for planning applications," *J. Transp. Eng.*, vol. 140, no. 9, 2014, Art. no. 05014004.

[13] S. C. Calvert, H. Taale, and S. P. Hoogendoorn, "Quantification of motorway capacity variation: Influence of day type specific variation and capacity drop," *J. Adv. Transp.*, vol. 50, no. 4, pp. 570–588, 2016.

[14] B. S. Kerner, S. L. Klenov, and M. Schreckenberg, "Simple cellular automaton model for traffic breakdown, highway capacity, and synchronized flow," *Phys. Rev. E, Stat. Phys. Plasmas Fluids Relat. Interdiscip. Top.*, vol. 84, Oct. 2011, Art. no. 046110.

[15] B. S. Kerner, "Failure of classical traffic flow theories: Stochastic highway capacity and automatic driving," *Phys. A, Stat. Mech. Appl.*, vol. 450, pp. 700–747, May 2016.

[16] M. Ameri, R. Moayedfar, and F. Jafari, "Determination the capacity of two-lane suburban roads with neural networks and effect of speed on level of service," *Eur. Transp. Res. Rev.*, vol. 5, no. 4, pp. 179–184, 2013.

[17] T. Q. Tang, W. F. Shi, X. B. Yang, Y. P. Wang, and G. Q. Lu, "A macro traffic flow model accounting for road capacity and reliability analysis," *Phys. A, Stat. Mech. Appl.*, vol. 329, no. 24, pp. 6300–6306, 2013.

[18] Y. S. Qian, X. M. Shao, J. W. Zeng, and M. Wang, "An improved cellular automaton model with the consideration of a multi-point tollbooth," *Phys. A, Stat. Mech. Appl.*, vol. 392, no. 23, pp. 5874–5878, 2013.

[19] X. Chen, L. Yu, X. Jia, and H. Gong, "Analytical procedures for estimating the capacity of the urban expressway section near off-ramps and on-ramps with a median exclusive bus lane," *J. Transp. Eng.*, vol. 140, no. 3, 2013, Art. no. 04013018.

[20] Z. He, L. Zheng, and W. Guan, "A simple nonparametric car-following model driven by field data," *Transp. Res. B, Methodol.*, vol. 80, pp. 185–201, Oct. 2015.

[21] W. Zhang, Z. He, W. Guan, and G. Qi, "Day-to-day rerouting modeling and analysis with absolute and relative bounded rationalities," *Transportmetrica A, Transp. Sci.*, vol. 14, no. 3, pp. 256–273, 2018.

[22] D.-F. Xie, Z.-Z. Fang, B. Jia, and Z. B. He, "A data-driven lane-changing model based on deep learning," *Transp. Res. C, Emerg. Technol.*, vol. 106, pp. 41–60, Sep. 2019.
[23] J. X. Shen, F. Qiu, R. Li, and C. Zheng, "An extended car-following model considering the influence of bus," *Tehnicki Vjesnik*, vol. 24, no. 6, pp. 1739–1747, 2017.
[24] C. F. Choudhury and M. E. Ben-Akiva, "Modelling driving decisions: A latent plan approach," *Transportmetrica A, Transp. Sci.*, vol. 9, no. 6, pp. 546–566, 2013.

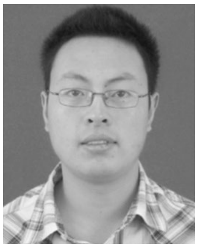

JINXING SHEN received the M.S. degree in transportation planning and management from Hohai University, in 2009, and the Ph.D. degree in transportation engineering from Southeast University, in 2015. He is currently a Lecturer with the College of Civil and Transportation Engineering, Hohai University. His research interest includes optimization of the multimodal public transportation systems.

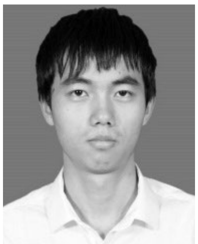

JUNJIE QI received the bachelor's degree in traffic engineering from Jiangsu University, in 2018. He is currently pursuing the M.S. degree with Hohai University, where he is also conducting a research on the planning and operation of public transit.

FENG QIU received the M.S. and Ph.D. degrees in transportation engineering from Southeast University, in 2014. He is currently pursuing the M.S. degree with the University of Victoria. His research interests include the areas of the multimodal traffic networks and information systems.

CHANGJIANG ZHENG received the Ph.D. degree in transportation engineering from Southeast University, in 2006. He is currently a Professor and a Ph.D. Supervisor with the College of Civil and Transportation Engineering, Hohai University. His research interests include different aspects of transportation planning and management.